COSMIC RAYS AT EXTREME ENERGIES

R.CESTER
Istituto di Fisica Sperimentale - Universitá di Torino e INFN
Via P. Giuria 1, Torino 10125, Italia
E-mail: Cester@to.infn.it

This paper briefly reviews the status of research on High Energy Cosmic Rays, in particular those populating the highest part of the energy spectrum ($E_{CR} > 510^{18} eV$) and believed to be of extra-galactic origin. An outlook on a new generation of experiments hopefully capable of answering open questions on production, acceleration and propagation mechanisms of these particles, concludes the paper.

1. Introduction

The discovery of Cosmic Rays (C.R.)dates back to the beginning of the 20th century. In 1936 the Nobel prize was awarded jointly to V. Hess [1] and to C.D.Anderson [2], to Hess for his 1912 experiments that proved the existence, in the highest layers of the atmosphere, of radiation coming from outer space, and to Anderson who in 1932 discovered, within the flux of secondary C.R. reaching earth, a new component of light, positive particles (positrons) soon after identified as the antiparticles of electrons.

After Anderson experiment, C.R. became a fertile ground of search for new particles with the rate of discoveries increasing rapidly as detection and measuring techniques improved, until, in the middle 1950s, it became possible to continue the search at particle accelerators. In the range of energy that can be reached at accelerators, C.R. are not competitive in the study of elementary particles and their interactions, however an energy window for the discovery of new phenomena still exists above 2×10^{15} eV.

A complementary and fundamental aspect in the study of C.R. is the measurement of the characteristics of the primary component reaching earth from outer space, to infer from these measurements informations on their sources. A major problem in the attempt to unravel this puzzle lies in the fact that we have for each incoming particle only three observables: mass, energy and direction, the measurement of which is far from trivial.

In this paper I will mainly concentrate on primary C.R. of energy above

10^{15} eV. At these energies it is not possible to measure directly the characteristics of the incoming particles that must be reconstructed from the study of secondaries reaching ground. A powerful handle to reconstruct energy and direction and to identify the type of primary particles comes from the study of electromagnetic air showers (EAS) generated from interactions of the incoming particles in the higher layers of the atmosphere and from the observation of muons from charged secondary particles decays, that penetrate down to ground. EAS were first detected in 1934 by B.Rossi [3] and systematically studied by P.Auger [4] who, with a comparatively large array of counters and good timing coincidence-circuits, succeeded in detecting showers of energy up to 10^{15} eV.

As experiments continued to yield evidence of the existence of C.R. of very high energy (up to 10^{20} eV and more), speculations on their sources, the acceleration processes, and on the effects of propagation through galactic and intra-galactic media were brought forward in an attempt to con struct a coherent picture of the phenomena.

This paper is organized in two parts. In the first I will attempt to follow the flow of ideas that in the last 50 years have contributed to what understanding we now have of the origin of high energy C.R.[5]. In the second, I will review experimental results and give an overview of the new more powerful generation of experiments exploring the highest energies, now in data taking or under construction.

2. C.R. from the Galaxy

The measured energy spectrum of C.R. is shown in Fig.1. For energies greater than 10^{10} eV, where the influence of the solar system can be ignored, and smaller than 10^{15} eV, the spectrum is well described by a power law:

$$\frac{dJ(E)}{dE} \propto E^{-2.7}\,, \tag{1}$$

The average concentration of elements in the Galaxy and in C.R. are quite similar; however there are some differences, the most pronounced one for light nuclei, Li, Be and Bo that are abundant in C.R. and almost absent in the galaxy. All the differences can be explained by the fact that C.R., while propagating in the galaxy, collide with particles (for the most part protons) of the interstellar medium (ISM). A quantitative analysis of the chemical and isotopic composition of C.R. reaching the earth indicate that the thickness of interstellar medium traversed by C.R. before reaching the earth is of the order of 5 to 10 g/cm^2 [6].

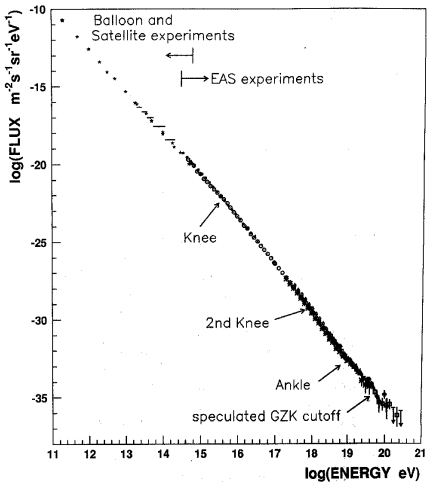

Figure 1. Measured C.R. spectrum.

C.R. appear to be isotropic and to carry an energy density of about 1 eV per cm^3, about twice that of star light. If they are uniformly distributed over the volume of the galaxy halo ($V_h \sim (10\ parsecs)^3 \sim 10^{68} cm^3$), the total energy carried by these particles is of the order of $W_{C.R.} \sim 10^{56}$ erg. Such huge energy implies that a powerful acceleration mechanism must be active in our galaxy.

2.1. *Fermi Acceleration mechanisms*

Fermi started studying C.R. in 1946. At the time it was already known that the majority of C.R were nuclear particles with a power-law energy spectrum with exponent -2.9, a value remarkably close to the present one.

From an estimate of the average density of ISM and the known cross-section for nuclear interactions, Fermi [7] calculated the lifetime of C.R. to be: $\tau_{nucl} \sim 7 \times 10^7$ years, much shorter than the universe lifetime. This implies continuous creation. If one assumes C.R. to be created at a constant rate, then the flux of such particles with age between t and $t+dt$ is:

$$dJ(t) \propto dt \times e^{-\frac{t}{\tau_{nucl}}}\ , \tag{2}$$

But how do these particles get their energy and what is the acceleration process that leads to a power-law spectrum? This law requires a very specific acceleration mechanism capable of indefinitely increasing the particle

energy. Fermi observed that, for the principle of equipartition of energy, this can be achieved in successive collisions with extremely large moving objects. The next step was that of identifying such objects. In Fermi's words: " **...the main process of acceleration is due to the interaction of cosmic particles with wandering magnetic fields which, according to Alfven, occupy the interstellar space..**" Alfven *clouds* drift through galactic space in stable configurations of highly irregular magnetic fields and " .. **to each line of force one should attach a material density due to the mass of the matter to which the line of force is linked...** ". The dimension of these clouds is of several light-years and their density is 10 to 100 times higher than that of the ISM they drift through at a velocity $V \sim 3 \times 10^6\ cm/sec$, ($\beta = \frac{V}{c} \sim 10^{-4}$). A particle trapped in one of these clouds, spirals around the field lines being elastically scattered when the magnetic field changes abruptly. With a simple analysis Fermi estimated that a particle fractional energy increases on average by: $\frac{\Delta E}{E} = \frac{4}{3}\beta^2$ in each collision with an Alfven cloud. After n collisions:

$$n \times \frac{\Delta E}{E} \sim \int_{E_0}^{E} \frac{dE}{E} = \int_{E_0}^{E} dlnE = ln\frac{E}{E_0} = n \times \frac{4}{3}\beta^2 \approx \frac{t}{\tau_{coll}}\beta^2\,, \quad (3)$$

where E_0 is the injection energy and τ_{coll} is the mean time interval between collisions. Combining the equation $E(t) = E_0 \times e^{\frac{t}{\tau_{coll}}\beta^2}$ with eq.2, the differential flux of C.R. as a function of energy is derived:

$$dJ(E) \propto dE \times E^{-\alpha} \qquad with \qquad \alpha = \frac{4}{3}\frac{\tau_{coll}}{\tau_{nucl} \times \beta^2} + 1\,, \quad (4)$$

As seen, the Fermi stochastic acceleration process leads naturally to a power-law spectrum; unfortunately the mechanism is highly inefficient, since the fractional energy increase in a collision is proportional to β^2 (hence the name *Fermi acceleration mechanism of second order*) and $\beta \approx 10^{-4}$.

It was only in the late 1970's that Fermi's basic ideas were extended and a more efficient *first order Fermi acceleration mechanism* was proposed. By that time supernova explosions had been studied in detail and it was suggested that C.R. in the galaxy could be generated and accelerated in this process[8]. In fig.2 the first order acceleration processes is compared to the second order one. The acceleration mechanism is basically the same but the particles are now accelerated in shock waves propagating out in the explosion with velocity $\beta \sim 0.1$, three orders of magnitude larger than that of Alfven clouds, and $\frac{<\Delta E>}{E}$ is proportional to β (*Fermi acceleration mechanism of first order*). It is estimated that C.R. emitted in a supernova explosion can reach energies up to $\sim 10^{13}$ eV and that multiple interactions

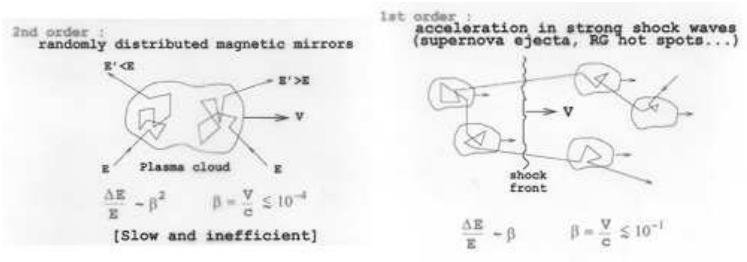

Figure 2. Fermi acceleration mechanism of second (left) and first (right) type.

of C.R.wandering through the galaxy, with supernova remnants can extend their energy up a few orders of magnitude[9].

2.2. *C.R. motion in the ISM*

Fig.3 shows an example of C.R. trajectories in the galactic magnetic fields which has a uniform component $B_0 \sim 2\mu G$ along the spiral arms and a component with random direction, B_r, of the same order of magnitude [10]. The C.R. particles spiral around the field lines with a Larmor radius:

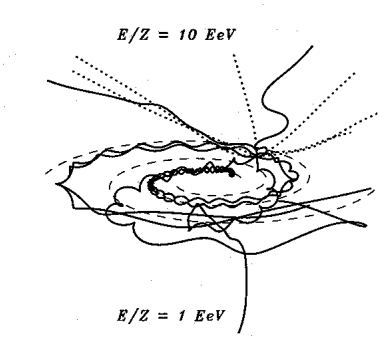

Figure 3. Simulation of C.R. trajectories in the galactic magnetic field; dotted lines are for particles with E/Z = 10^{19} eV, full lines for particles with E/Z = 10 ^{15} eV

$$r_L(pc) = \frac{E_{15}}{B_0(\mu G)Z}\,, \tag{5}$$

(with E measured in (10^{15} eV) and r_L measured in parsecs) and scatter on the random irregularities. The long random walk of C.R. in the galaxy

explains why, when reaching earth, C.R. are isotropically distributed. This effect is, of course, less pronounced for C.R. of higher energies (fig.3).

3. From Galactic to Extra-Galactic C.R.

In fig.4 the flux of C.R. with $E > 10^{13}$ eV, as measured by recent experiments, is plotted as a function of energy. The flux is rescaled by E^3 to enhance the features showing-up above 10^{15} eV[11]. As we have seen, for C.R. energies up to 10^{15} eV the differential spectrum is described by a power law $\frac{dJ(E)}{dE} \propto E^{-\alpha}$ with $\alpha = 2.7$. The first anomaly (*the knee*) appears at $E \sim 3 \times 10^{15}$ eV where α changes from 2.7 to ~ 3, followed by a second change in steepness (*the second knee*) at $E \sim 4 \times 10^{17}$ eV where α reaches a value ~ 3.3. At $E \sim 5 \times 10^{18}$ eV the spectrum shape changes again,

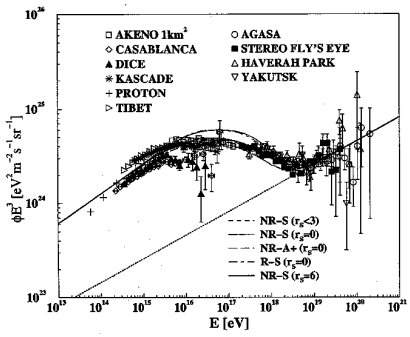

Figure 4. Measurements of the energy spectrum of C.R. (rescaled by a factor E^3). The dotted line shows the onset of an extragalactic component. Also shown are predictions of transport calculations performed using different galactic models.

and can be fit to a power law with $\alpha \sim 2.7$ (*the ankle*). The *knee* structures are explained by the conjecture that for E/Z above a threshold value, C.R. start escaping from the Galaxy halo, causing the observed reduction in their local density. The phenomenon has been successfully modeled with detailed simulations of C.R. transport through the magnetic fields permeating the galaxy, assuming a realistic distribution of supernova sources[12]. Since the magnetic field effect depends only on E/Z, lighter nuclei will start escaping first so that we expect to observe a change in composition as the energy increases. Fig.5 shows how the measured composition evolves with energy. Recent results appear to agree well with the prediction of the model. Above the *ankle* C.R. originating in the Galaxy are no longer

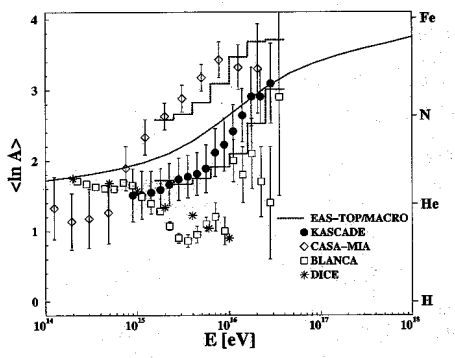

Figure 5. Measured composition ($< ln\ A >$) as a function of energy compared to the result of a transport calculation (full line).

confined and the hardening of the spectrum suggests the onset of a new component probably of extra-galactic origin. The C.R. spectrum extends up to energies $\geq 10^{20} eV$ and the crucial issue becomes that of identifying sources where energies of such magnitude could be reached.

4. Ultra High Energy Cosmic Rays (UHECR)

As we see in fig.4 the flux of C.R. cuts off at about 10^{20} but it is not clear if this is due to a real effect or a consequence of the limited aperture of experiments at an energy where the flux is at most of one event per $sterad \times km^2 \times century$. Even with the new large-aperture experiments under construction, if a cut-off is observed, we will need auxiliary informations to establish if this is due to lack of high-power sources or to the degrading effects of interactions in the inter-galactic medium, discussed in the next section.

4.1. *The Greisen-Zatseping-Kuz'min (GZK) effect*

In 1965 Penzias and Wilson[13] discovered quite accidently that the Universe is uniformly filled with soft electromagnetic radiation, the so called Cosmic Microwave Background (CMB) with a blackbody spectrum peaked at 6×10^{-4} eV and a density of about 400 photons/cm^3. The existence of CMB had actually been predicted as a relic of an early-universe time when H atoms were formed and neutral matter decoupled from radiation [14].

Soon after the discovery, Greisen and independently Zatseping and Kuz'min [15] noticed that C.R. will interact with these CMB photons and

loose energy in the process. These authors were referring specifically to a highly inelastic reaction:

$$p + \gamma \rightarrow \Delta^+ \rightarrow \pi^+(\pi^0) + N(P)\,, \tag{6}$$

with a threshold at $\sim 4 \times 10^{19}$ eV and an energy loss of $\sim 20\%$ of the proton energy. Other reactions are:

$$p + \gamma \rightarrow P + e^+ + e^-\,, \tag{7}$$

with a threshold at $\sim 10^{18}$ eV and an energy loss of only $\sim 0.1\%$ and, for heavy nuclei, photo-disintegrations and pair production, with the largest energy loss for the process:

$$A + \gamma \rightarrow (A-1) + N\,, \tag{8}$$

These predictions seemed to contradict the findings of the Vulcano Range experiment [16] that in 1962 had detected an event with energy E $> 10^{20}$ eV. However this apparent contradiction could be explained if the source of such event was at a relatively small distance from our observation point. Recent calculations, which include the effect of all components (microwave, infrared and radio) of intergalactic background radiation, have determined the energy dependence of the attenuation length of different C.R. particles[5] (see fig.6) and indicate that, if the Vulcano Range event was initiated by a primary proton,it must have come, with high probability, from a distance < 50 Mpc. As we will discuss in detail in the second part of this paper, after 45 years of the detection of the Vulcano Range event and in spite a wide experimental effort, we still do not have a reliable estimate of the flux of events with energy $\geq 10^{20}$ eV. It is hoped that the new generation of experiments will clarify the matter and identify the sources of such events.

4.2. *The sources*

There are two classes of models to explain the existence of C.R. with E$> 10^{19} eV$ (UHECR). The first one (Bottom-up models) assumes that they are produced and accelerated in astronomical objects where catastrophic processes with large energy transfers are taking place. The second one (Top-down models) assumes that UHECR get their energy from the decay of some yet undiscovered high-mass particle.

4.2.1. *Bottom-up models*

I discuss first Bottom-up models as they are less controversial. In one scenario the acceleration process occurs in shock waves projected out in

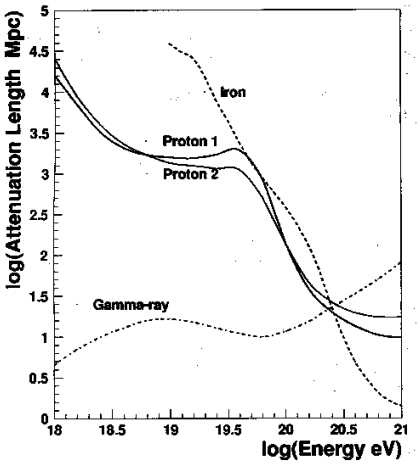

Figure 6. Attenuation length of proton, iron and gamma-ray primary C.R. in the intergalactic background radiation.

extra-galactic astronomical explosions far more powerful than the galactic supernova ones, and that UHECR acquire energy through a Fermi mechanism where the relevant parameters reach extreme values. A simple analysis helps identifying such parameters and their range of values[17].

To be effectively accelerated particles must be trapped in the magnetic field (B) of the acceleration region, hence the characteristic length (L) of this region must be larger than twice the particle Larmor radius r_l:

$$L(pc) >> 2 \times r_l(pc) \approx 2 \times \frac{E_{15}}{Z \times B_T(\mu G)}\,, \tag{9}$$

where B_T is the component of the magnetic field normal to the particle direction and E_{15} is the particle energy in units of 10^{15} eV. Moreover, as we have seen, in a first order Fermi-type process, the energy increment depends linearly on the velocity β of the shock wave, so that we may expect the maximum energy attainable to be:

$$E_{15} = k\frac{B_T(\mu G) \times L \times Z \times \beta}{2}\,, \tag{10}$$

with k always < 1. The relevant quantities in this problem are therefore the magnetic rigidity $\mathrm{B}_T \times L$ and the velocity of the shock, β. Particles may also be accelerated to high energy directly by extended electric fields. As is well known, such extended electric fields can be generated in the rotation of magnetized conductors. In rapidly rotating neutron stars, the conditions

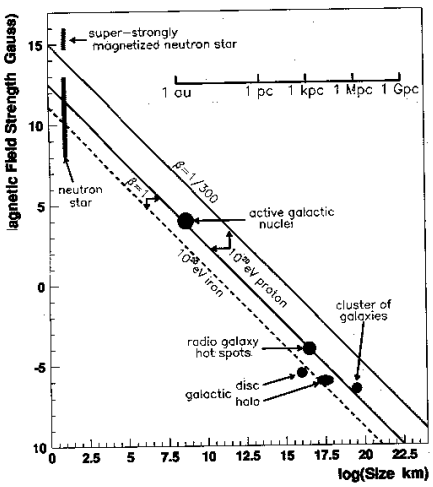

Figure 7. Size and magnetic-field strength of acceleration sites where CR could reach energies above $10^{20}eV$. The two lower lines refer to ultra-relativistic shock waves ($\beta \sim 1$) (full line for protons and dotted line for iron nuclei), the upper line refers to protons in shock waves with $\beta = \frac{1}{300}$. Drawn on the plot are candidate astronomical sites.

are met for such an acceleration mechanism to take place. In Fig.7 known astronomical objects where UHECR could be produced and accelerated, are drawn on a log/log plot of B vs L [18]. Only in regions above the diagonal lines can particles be accelerated to $E \geq 10^{20}eV$.

The lower-right part of the plot is populated by extra-galactic objects. I list some of the most interesting below, referring[5] the reader to the specialized literature for a deeper understanding of their characteristics.

Radio-Galaxies Hot Spots are gigantic jets ejected at relativistic speed from an Active Galactic Nucleus (AGN) where shock waves of few kiloparsec, with magnetic fields up to hundreds of $\mu Gauss$ could be generated.

Cosmological Gamma Ray Bursts (GRB) are thought to be produced when massive stars or binary systems collapse into black holes. Energy is released almost instantaneously in an expanding fireball where the γ emitting region moves relativistically with a Lorentz factor of several hundreds. It is conjectured that in such environment, protons are accelerated to the highest energies, through a second order Fermi mechanism, within regions expanding with a velocity V $\sim c$ in which strong, random magnetic-fields are thought to be present. A common origin for the two phenomena is suggested by a remarkable coincidence between the energy flow of UHECR

and GRB[19]. These sites and AGNs are favored candidates as sources of protons of energies up to 10^{21} eV.
Colliding Galaxies: when two galaxies collide, the converging flows could contain shock fronts capable of accelerating iron nuclei up to 10^{20} eV.
Clusters of galaxies: particles could be accelerated to high energy by accretion shocks formed by the in-falling flow toward a cluster of galaxies.
Nearby Galaxies: It can not be excluded that UHECR come from 'normal' galaxies where the level of activity, star formation and magnetic fields are higher than in our galaxy. Then the C.R. flux at emission should be proportional to the distribution of luminous matter and their mass composition similar to the one of our galaxy.

In the upper-left part of fig.7 are galactic **Neutron stars** where rapidly rotating, strong magnetic-fields can generate electromotive forces capable of accelerating Iron nuclei to ultra-high energy[20].

I conclude by noting that what we will observe with our experiments depends crucially not only on the source accelerating power but also on its distance (d) from the solar system and on the distribution of sources in the universe. Particles coming from objects close-by, on the universe scale of distances ($d \leq 50Mpc$), will not be substantially affected by the interaction with the CMB even if their energy is above the GZK threshold. The hypothesis that these objects are sources of UHECR can then be tested by measuring the pointing direction of the incoming particles which should correlate with the position of the source since over distances d $\leq 50Mpc$ particles will not be significantly deviated by the rather weak intergalactic magnetic-fields. If, on the other side, the sources are distant objects ($d >> 50Mpc$), we do not expect to detect particles with energy above $\sim 6 \times 10^{19}$ eV irrespective of their energy at the source. Moreover since particles of this energy have attenuation paths in the inter-galactic media of $\sim$ 1000 Mpc (see fig.4) they will wonder around, scattered by magnetic fields irregularities. We therefore expect that when reaching our galaxy they will have lost memory of the initial direction. It is also very important to determine the mass of the incoming particles, protons or heavier nuclei, since this might help differentiating between possible sources.

4.2.2. *Top-down models*

Far more speculative are the models that assume that UHECR come from the decay of super-heavy particles predicted by theory. First because no experimental hint of such particles exists so far, and second because to

explain the observed flux of UHECR, their density and decay life-time must be chosen 'ad-hoc'. A common feature is that, given their large mass, they would accumulate in the galaxies halo so that their decay products would reach the earth unaffected by CMB. Candidate objects are: early-universe relic super-heavy particles, topological defects created in the phase-transition of the early universe, magnetic monopoles and supersymmetric hadrons[5]. A strong signature for some of these models is that γs and neutrinos would account for a large fraction of the decay products reaching the solar system.

Finally, I touch on yet an other model[21] that would predict a large flux of high energy γ rays and neutrinos from the production-decay chain:

$$p + ... \rightarrow \nu + ... \quad with \quad E_\nu \sim 4.10^{21}\,, \tag{11}$$

$$\nu + \bar{\nu}_{rel} \rightarrow Z^0 \rightarrow kP + n\pi^0 + m\pi^{+-} .... \rightarrow k \times P + 2n \times \gamma + 3m \times \nu..\,, \tag{12}$$

The Z^0 decay branching ratios are well known and a ratio of k/n/m/= 2/10/17 is expected. The high-energy incoming neutrino interacts resonantly with an anti-neutrino of the *cosmic neutrino background* (a relic of the early stages of the universe) to form a Z^0 particle. Given the values of the neutrino and of the Z^0 masses, the energy of the incoming neutrino is derived by simple kinematics. Once again the major problem here is that of finding a source sufficiently powerful to accelerate the particles that initiate the production-decay chain.

5. Experimental Overview

High energy C.R. entering the atmosphere undergo nuclear interactions producing a large number of hadrons. While propagating through the atmosphere, particles interact repeatedly producing a high multiplicity cascade. The main components reaching ground are the barionic one, in a small angular cone approximately along the direction of the incoming C.R. and, distributed over a wider area, muons from charged π decays and electrons and γs in electromagnetic showers.

Electromagnetic showers are initiated by the decay of π^0's to 2γs which undergo conversion to e^+e^- pairs; electrons, in turn, emit γs in the *Bremsstrahlung* process. The interplay of the two processes leads to particles multiplication and to the degrading of particles energy until a point is reached where the electron energy falls below the *Bremsstrahlung* threshold and the multiplication process stops. Electrons loose their residual energy interacting with atoms and molecules of the atmosphere and the shower

tapers off. The shower can be parametrized by the atmospheric depth of the first interaction X_0, the depth at maximum, X_{max}. and the number, N_{max} of electrons at X_{max}.

5.1. *Detection and Analysis methods*

The properties of the UHECR have been studied in two ways: a) with large arrays of ground-based detectors that measure the flux of muons and/or the energy carried by the electromagnetic component and b) with optical detectors measuring the yield of fluorescence photons emitted along the electromagnetic shower path[22].

5.1.1. *Arrays of Surface Detectors (SD)*

The use of these detectors has two major advantages: a) they are little affected by external conditions, and therefore can run continuously and, b) they can be built of identical modules that, to instrument large areas, must be simple, low cost and stable. Two types of modules have been frequently used: a) scintillator/absorber sandwiches to count muons (μ *detectors*), and b) water Cherenkov tanks to measure the energy deposited by electrons and muons (H_2O *Cher.*). The main disadvantage of this technique lies in the fact that all informations on the characteristics of primary C.R. come from a snapshot of the shower at ground level. As a consequence the validity of the results are strongly dependent on the ability to model accurately the development of showers through the atmosphere.

Events are accepted if they meet a trigger condition that requires a minimum number of modules to have fired (typically 3 or 4). Hence the energy range of acceptance of the detector is bound on the low side by the choice of the array lattice spacing. On the upper side it is the total exposure, the product of the detector aperture times the effective running time, that sets a bound to the energy range.

Measurement of the primary CR direction: The direction of the axis of the shower measures the primary CR arrival direction. If at least three non-collinear ground stations record the shower, its direction can be computed using detectors position and arrival times.

Energy measurement: the determination of the primary C.R. energy. is based on the measurement of a single parameter, the signal density ρ at an optimal distance l from the shower core (typically 500 to 1000 m), This method [23] relies on the fact (born out by simulations) that the value of $\rho(l)$ correlates strongly with the primary energy, weakly to the particle identity.

and is quite insensitive to fluctuations in the development of the shower. The weak point of the method lies in the fact that the conversion factor between $\rho(l)$ and primary energy must come from simulations.
Identification of the primary: for each event the most effective indicators of the primary identity are the rise-time of the signal detected far from the shower core and the muon content of the showers. As an example, a Fe nucleus will produce $\sim 70\%$ more muons than a proton of the same energy. Showers initiated by γs will have a low muon content.

5.1.2. *Fluorescence Fly's Eye Detectors (FD)*

When a Cosmic Ray interacts in the upper levels of the atmosphere, originating a shower that propagates down to earth, the charged particles in the shower excite the Nitrogen molecules and ions which decay emitting light in the near-ultraviolet wavelength range. The process has a very low efficiency with only $5{\times}10^{-5}$ of the shower energy carried by fluorescence photons. The light is emitted isotropically with an yield proportional to the particle ionization loss, hence, for relativistic particles, to track length, and almost independent of the atmospheric depth. Detecting this signal one can perform a measurement of the shower energy profile using the atmosphere as a calorimeter. The signal is however so weak that this technique can only be applied to study very high energy showers when background light levels are low, typically in clear, moonless nights.

Each Fluorescence Detector *eye* is built out of telescopes. The conceptual scheme of a telescope is very simple(see fig.8): a light collecting element (i.e. a spherical mirror) defines the aperture and focuses the light collected onto a camera, an array of phototubes positioned approximately on the mirror focal surface. To reduce background, the incoming light is filtered to cut out the unwanted components of the night-sky light spectrum. As the shower comes into the field of view of one telescope, an image is formed on the camera that tracks the trajectory of the shower as it develops through the atmosphere. From each PM, amplitude and timing of the signal are read out. From these data the following characteristics of the shower can be reconstructed:
Direction of the shower axis. The reconstruction of the shower geometry starts with the determination of the shower-detector plane (SDP) obtained by a fit to trial configurations of the triggered pixels directions, weighted by signal amplitude. A precision of $\sim 0.25^0$ on the direction of the normal to the SDP can be achieved. If the shower is detected by two eyes

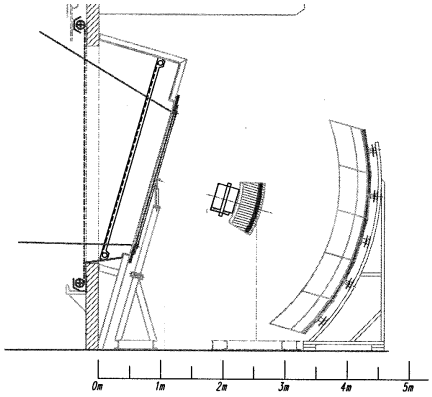

Figure 8. Drawing of a Fluorescence Detector telescope for the Auger experiment.

(*stereo event*), the direction of the shower is precisely reconstructed from the intersection of the SDP's determined from the two eyes. For *monocular events*, that is for events seen by one eye only, it is not always possible to reconstruct unambiguously the direction of the shower axis within the SDP.
Energy measurement: The light yield reaching the detector, scaled to ionization energy and corrected for geometrical factors and for the losses due to absorption and scattering in the atmosphere, measures the shower-energy: It gives a lower bound to the primary energy since $\sim 10\%$ of the shower energy is carried by neutral particles and part is lost in the ground. This effect can be corrected for without introducing a large systematic error. Dangerous sources of systematics are: a) the yield of fluorescence light emitted by Nitrogen and its dependence on the atmosphere parameters is still not precisely known[24], b) the presence of a Cherenkov-light component in the detected signal will affect the energy integral and distort the shower profile[5]. The Cherenkov light beamed directly into the detector acceptance can be estimated from the known angular distribution of electrons in the shower, and subtracted out. It is however more difficult to evaluate the fraction of Cherenkov light scattered into the detector acceptance by the aerosol molecules in the atmosphere,
c) an insufficient understanding of the characteristics of the atmosphere along the light path between the shower and the detector is potentially the worst cause of systematic errors in the determination of the shower parameters. An accurate monitoring of the atmosphere parameters and of the aerosol component is therefore essential.

Identification of the primary: The position of the shower maximum (X_{max}) is a good indicator of the nature of the primary particle. It changes over a range of 100 gm/cm^2 for nuclei of A=1 to A = 56 and, of course, is quite different for γs and weakly interacting particles. To have a reasonable sensitivity to the nuclear mass one needs to measure the position of shower maximum to a precision of $\leq$ 20 gm/cm^2.

It should be noted that X_{max} does not depend only on A but also on the shower energy and on the hadronic interaction characteristics. It can be approximated by the expression[5]:

$$X_{max} = (1 - B).\chi_0.(ln(\frac{E}{\epsilon}) - < lnA >) \,, \tag{13}$$

where B (always < 1) carries the information about the hadronic interactions cross sections and particles multiplicities. χ_0 and ϵ are radiation length and critical energy of air. The rate of change of X_{max} with the logarithm of energy (*Elongation rate*):

$$D_e = \frac{\partial X_{max}}{\partial lnE} = (1 - B).\chi_0.(1 - \frac{\partial < lnA >}{\partial lnE}) \,, \tag{14}$$

(or the more commonly used $D_{10} = 2.3D_e$), is constant if the mass compositions is constant, in which case the only parameter to be determined is B. A change in D at a given energy, signals a change in the average mass composition at that energy

5.2. *Experimental Results*

In Table 1 I have summarized some of the characteristics and results of UHECR experiments[25,26,27,28,29,30]. All entries refer to experiments located in the northern hemisphere, except Auger South. I have omitted the only other southern experiment, SUGAR[31] - Sidnay University Giant Array - which yielded few results.

There is not a good agreement in the measured energy spectrum between experiments using ground arrays (1st part of the Table) and experiments using fluorescence detectors (2nd part of the Table) as shown in fig.9. Over the full range of UHECR energies, the flux of AGASA is higher than the flux measured by the FD experiments. It has been estimated that an energy miscalibration of $\sim$ 30% [32]could explain the difference. Also the rate of events above $E > 10^{20}$ eV disagrees. Summing separately over the two sets of experiments, we find for the ratio of the (*number of events with energy above* 10^{20} *eV/exposure*), respectively (2.26 ± 0.54) $(m^2 \times sterad \times sec)^{-1}$ for SD and $(0.26^{+0.25}_{-0.14})$ $(m^2 \times sterad \times sec)^{-1}$ for FD. If we assume that

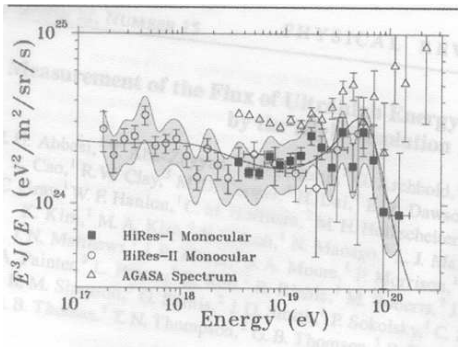

Figure 9. Comparison between the energy spectrum of UHECR as measured by Agasa, and the combined HiRes-I and HiRes-II results. The shaded band reflects the estimate of systematic errors by HiRes.

this is due to a systematic error on the energy measurement, rather than to a $\sim 3.5\sigma$ statistical fluctuation, we would be tempted to privilege the FD result since it depends less on simulations. In this case one could conclude that there is evidence of a GZK cutoff. However, as we saw, the FD energy measuring technique has its own problems. Moreover, at the highest energies, there is considerable uncertainty on the HiRes aperture[33]. All experiments have searched for anisotropies in UHECR incoming directions. AGASA has reported small-angle correlations between doublets (5) and triplets (1) of events[34]. However a recent analysis [35] has cast doubts on the significance of the signal. Other reported correlations of UHECR incoming directions with known astronomical objects have not, so far, found

Table 1. Experimental overview: Volcano Range (V.R.),Haverah Park (H.P.),AGASA and Yakutsk (Ykt) use Ground Arrays while Fly's Eye (Fleye) and Hires use Fluorescence Detectors).

Exp.	Status	Detect type	Exposure (10^{16} $m^2.ster.s$)	SD Area (Km^2)	FD eye Aperture $\Delta\phi.(\theta_1-\theta_2)$	N_{events} ($>10^{19.6}$ /$>10^{19.8}$ eV)	N_{events} ($>10^{20}$ eV)
V.R.	ended	μ	0.2	8		6/-	1
H.P.	"	H_2OCh	0.73	12		27/-	4
AGASA	"	μ	5.1	100		72/24	11
Ykt	Data	μ	$\sim$1.5	18 (10)		14/-	1
FlEye	ended	FD mn	2.6			24/-	1
"	"	FD st	0.46			2/-	0
HiresI	Data	FD mn	7.6		$2\pi(3^0-17^0)$	-/10	2
"II	"	FD mn	1.0		$2\pi(3^0-31^0)$	-/3	0
Aug.S	Constr.	Hybrid		3000	$\pi(1.7^0-31.3^0)$	-	$\sim$30/yr
T.A.	Constr.	Hybrid		760	$2\pi.(2^0-32^0.)$	-	$\sim$ 10/yr

confirmation.

The mass assignment of UHECR is also an open question, with different methods giving different answers and the conclusions being based on shower development models. The *elongation rate* by FD detectors suggests that UHECR are predominantly protons. The same conclusion is reached measuring the fluctuations in X_{max} that should be larger for lighter nuclei. In contrast, AGASA, from muons densities at ground, finds that a consistent fraction of UHECR are Fe nuclei[32].

Attempts have also been made to set limits to the fraction of γs in the primary flux at and above the GZK limit. At present the limits are still rather loose due to the small number of events. Simulations [36] show that *elongation rate* is a sensitive tool to detect very high energy γs and will certainly be exploited by future experiments.

5.3. *The new generation of experiments*

In the last two raws of Table 1 are listed some of the characteristics of two experiments now under construction that will, hopefully, soon produce data capable of substantially improving our understanding of UHECR. These experiments were designed when it was already clear that two essential conditions should be met: a) the aperture of the detector systems had to be large enough to collect a statistically significant number of events in the GZK cutoff energy region (possibly within the life-span of a physicist), and b) guarantee control of the systematics on energy measurements.

The design of the **Auger Observatory** includes two equal sites, one in the South and one in the North hemisphere to provide full sky coverage. Construction of the South Observatory, situated in the district of Malargue, Argentina, (35.1^0 - 35.6^0 South, 69.0^0 - 69.6^0 West) is well underway, while decisions on the Northern site are still pending. The experiment is built as a *Hybrid Detector* with two components: a) a 3000 Km^2 SD array of 1600 H_2O Cherenkov counters, distributed over a hexagonal lattice with 1.5 Km spacing between modules and, b) 4 fluorescence *eyes* overlooking the SD array. The number of FD eyes and their location on the site are chosen so that all showers of energy $\geq 10^{19}eV$ that hit the SD, will be seen by at least one eye, when the FD is operational. Details on the detectors characteristics can be found in a recent paper [37].

As we have seen, a ground array has 100% duty cycle while the duty cycle of FD's is not more than 10%. Therefore the merit of an hybrid detector is that of providing a subset of *golden events* that can be used to

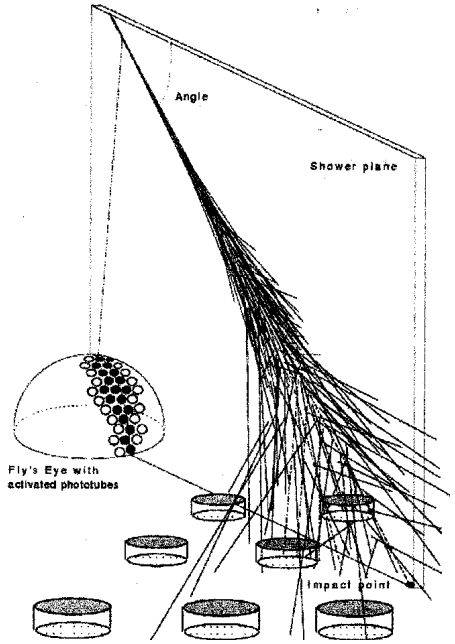

Figure 10. Artist view of an Hybrid detector.

understand the systematics of the energy and direction measurements of both SD and FD. The cross-check is particularly important if looked upon as a training procedure that will validate the measurements done on the majority of the events where only SD information is available. Furthermore, for this subset of events, the identity of primary particles can be more reliably determined exploiting the combined set of tools; X_{max} from FD , μ density, signal rise-time etc. from SD data.

At the time of writing ~ 600 H_2O Cherenkov detectors have been deployed and are routinely taking data, as are 2 of the 4 FD eyes. It is anticipated that by the middle of 2005 a set of data equivalent to that collected in 12 years running of AGASA, will be available.

The Telescope Array (TA) Hybrid Detector, the first stage of a program to explore the north-hemisphere sky, is under construction in the West desert of Utah (USA). The SD Array will have 576 scintillator detectors for muon counting, spaced by 1.2 Km, and will be surrounded by three FD eyes of 40 telescopes each, with full azimuth coverage. It is expected that data taking will start in 2007.

5.4. *Future Outlook*

Programs for the next two decades include: Auger North, the Fluorescence Telescope Array and EUSO, the Extreme Universe Space Observatory.

The base-line design of **Auger North** foresees an observatory with the same area and the same detector characteristics as Auger South to allow a direct comparison of data from the two sky hemispheres. The results obtained in Auger South will however undoubtedly have an impact on the final design of Auger North.

The final goal of the **Telescope Array** collaboration is that of building a very large fluorescence detector[38] system covering an area of about 200 km^2 with 10 eyes at a distance of 30 to 40 Km from each other. The basic construction characteristics of one *eye* are the same as in the hybrid detector now being built in Utah, but improvements on the optics and on read-out electronics are proposed. The fate of Auger North and of the fluorescence TA, both now stalled by funding problems, will in the end depend on the physics scenario that Auger South and Hybrid TA will uncover in the next few years.

By far more innovative is the **EUSO** experiment which has been designed to measure EAS with a satellite-borne fluorescence detector [39]. A space mission requires a compact, radiation resistant detector with low power consumption, and capable to operate reliably over a long period of time. The present design of the detector, based on an aggressive R.&D. program, features a wide angle ($\pm 30^0$), high resolution ($\sim 0.1^0$) telescope. This resolution is reached with a fine segmentation of the detector area ($> 10^5$ pixels) and corresponds to a spatial resolution on the ground of $\sim 1Km$ and a resolution on the primary C.R. direction of $\sim 1^0$, comparable to that of ground-based detectors. The FD will be installed in a payload facility aboard the International Space Station (ISS) and will then look down at the earth atmosphere from a ~450 Km high ISS orbit. The geometrical aperture of ~500000 km^2 sr will be reduced by a factor ~ 10 due to the limited observational duty cycle. Even so it will be about ~ 7 times that of the Auger South ground-array, with uniform sky coverage. Uniform sky coverage is very important in the study of large scale anisotropies associated with the galactic structure and super-galactic plane. Euso will monitor an atmospheric volume of ~ 1500 Giga-tons of air and therefore has a strong capability to detect down-going UHE neutrinos interacting in the atmosphere or up-going ones interacting in the upper layers of the earth crust.

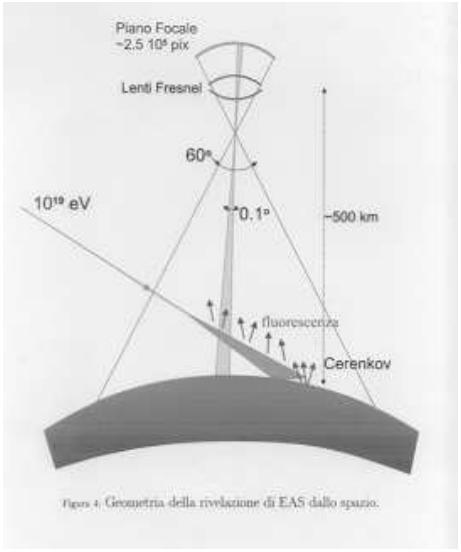

Figure 11. Schematic view of Euso experiment.

There are a number of reasons why it is important to detect UHE neutrinos: a) they are the only messengers from optically thick sources, opaque to other particles and b) they will provide a signature for sources where high energy π meson are produced, since the charged pion decay-chain ends into 3 neutrinos (ν *and* $\overline{\nu}$s) and one $e^{\pm}$. If nothing else, we should see neutrinos from proton interactions on CMB. It should also be noted that, due to vacuum oscillation, if neutrinos are produced in distant objects, they should be almost equally distributed between the three flavors when they reach earth. Auger[40] and the large FD of TA[41] both claim to be, under favorable neutrino flux conditions, sensitive to neutrino-initiated EAS, however, a systematic study of these events with an adequate statistics, will probably have to wait for EUSO. Unfortunately at present the space mission is uncertain and might be delayed until the end of the next decade.

References

1. V.Hess, *Phys.Zs.* **13**, 1084 (1912).
2. C.D.Anderson, *Phys.Rev.* **43**, 491 (1932).
3. B.Rossi, *Phys.Rev.* **45**, 212 (1934).
4. P.Auger, *Rev.Mod.Phys.* **11**, 288 (1939).
5. For a complete review of the subject and list of references see M.Nagano and A.A. Watson*Rev.Mod.Phys* **72**, 689 (2000).

6. V.S.Berezinsky et al.*Astrophysics of Cosmic Rays, North Holland,Amsterdam* (1990).
7. E.Fermi, *Phys.Rev.* **75**, 1169 (1949) and *N.C. Suppl.* **6**, 317 (1949)
8. R.D.Blanford and J.P.Ostriker *Astrophys.J.Lett.***221**, L29 (1978)
9. W.H.Ip and W.I.Axford *Proceedings of the International Simposium on AstrophysicalAspects of the MostEnergetic C.R.* edited By M.Nagano and F.Takahara (W.S. Singapore) 273 (1991)
10. D.Harari et al., *JHEP* **08**, 022 (1999).
11. E.Roulet et al., *JHEP* **0212**, 032 (2002).
12. J.Candia et al., *JHEP* **0212**, 033 (2002).
13. A.A.Penzias and R.W.Wilson, *Astrophys.J.* **142**, 419 (1965).
14. R.H.Dicke et al., *Astrophys.J.* **142**, 414 (1965).
15. K.Greisen, *Phys.Rev.Lett.* **16**, 748 (1966) and Z.T.Zatsepin and V.A.Kuz'min *Exsp.Teor.Phys.Pis'ma Red.* **4**, 144 (1966)
16. J.Linsley et al., *Phys.Rev.Lett.* **10**, 146 (1963).
17. L.Drury, *Contemp.Phys.* **35**, 232 (1994).
18. A.M.Hillas, *Ann.Rev.Astron.Astrophys.* **22**, 425 (1984).
19. E.Waxman, *Phys.Rev.Lett.* **75**, 386 (1995).
20. A.V.Olinto et al. *Proceedings of the 26tth ICRC, Salt Lake City* vol.**4**, 361 (1999)
21. S.Yoshida et al., *Phys.Rev.Lett.* **81**, 5505 (1998).
22. A.N.Bunner,Ph.D.thesis (Cornell University) 1964
23. A.M.Hillas, *Acta Phys.Scient.Hungar.* **29**, Suppl.3, 355 (1970).
24. M.Nagano et al., *Astropart.Phys.* **22**, 235 (2004).
25. J.Linsley (Volcano Range), *Proceedings of the 8tth ICRC, Jaipur* (Tata Inst.for Fundam.Research) vol.**4**, 77 (1963)
26. LaurenceM.A. et al.(Haverah Park), *Phys.Rev.Lett* **63**, 1121 (1989).
27. M.Takeda et al.(AGASA), *Astropart.Phys.* **19**, 447 (2003).
28. V.P. Knurenko et al.(Yakutsk), *ArXiv:astro-ph.*/0411484 v1 (17 Nov 2004).
29. D.Bird et al.(Fly's Eye), *Astropart.J.* **511**, 739 (1999).
30. R.U.Abbasi et al.(HiRes), *Phys.Rev.Lett.* **92**, 151101-1 (2004).
31. L.J.Kevley et al.(SUGAR), *Astropart.Phys.* **5**, 69 (1996).
32. A.A. Watson, *Proceedings of the conference on 'Thinking and Observing the Universe, Sorrento-Italy*, 22 (Sept.2003).
33. E.Bergman et al., *Proceedings of the 28th ICRC, Tsukuba* **1**, 397 (2003).
34. M.Teshima et al., *Proceedings of the 28th ICRC, Tsukuba* **1**, 437 (2003).
35. C.B.Finley and S.Westerhoff, *ArXiv:astro-ph.*/0303484
36. D.Heck (private communication]
37. The Auger Collaboration, *Nucl.Instr.and Meth.A* **523**, 50 (2004).
38. M.Sasaky, *Proceedings of the 285th ICRC, Durban* **5**, 369 (1997).
39. Euso Proposal
40. K.S. Capelle et al. *Astropart.Phys.* **8**, 321 (1998).
41. M.Sasaki et al., *ArXiv:astro-ph.*/0204167, 15 Jul 2002